Determining how human mesenchymal stem cells change their degradation strategy in response to microenvironmental stiffness

Maryam Daviran, Jenna Catalano, and Kelly M. Schultz[*]

Department of Chemical and Biomolecular Engineering

E-mail: kes513@lehigh.edu

Phone: 01 610 758 2012

Table S1: Changes in the wt% of the MMP-degradable peptide and the overall hydrogel with different thiol:ene ratios.

R = thiol:ene	0.55	0.65	0.7	0.75	0.85	1
Peptide cross-linker (mM)	3.3	3.9	4.2	4.5	5.1	6
Peptide cross-linker (wt%)	0.43	0.51	0.55	0.59	0.67	0.78
$wt\%_R - wt\%_{R=0.55}$	0	0.08	0.12	0.16	0.24	0.35
$\frac{wt\%_R - wt\%_{R=0.55}}{wt\%_{R=0.55}} \times 100$	0	8	12	16	24	35

Table S2: Measured modulus ($G'_{unswollen}$), calculated cross-link density (ρ), ideal cross-link density if 100% of cross-links form (ρ_{ideal}) and cross-linking efficiency, ϵ, for unswollen hydrogels with different thiol:ene ratios from bulk rheology measurements. The critical fraction of the PEG reaction sites needed to form a gel, p_c, calculated from Flory-Stockmayer theory is also provided.

R = thiol:ene	0.55	0.65	0.7	0.75	0.85	1
$G'_{unswollen}$ (Pa)	270	720	1000	1140	1540	2140
ρ $(m^{-3}) \times 10^{-23}$	0.65	1.7	2.4	2.7	3.7	5.2
ρ_{ideal} $(m^{-3}) \times 10^{-23}$	3.9	4.7	5.1	5.4	6.1	7.2
$\epsilon = \frac{\rho_{bulk measurments}}{\rho_{ideal}}$	0.17	0.36	0.47	0.5	0.61	0.72
$\epsilon \times 100$ (%)	17	36	47	50	61	72
p_c	0.41	0.46	0.48	0.5	0.53	0.57

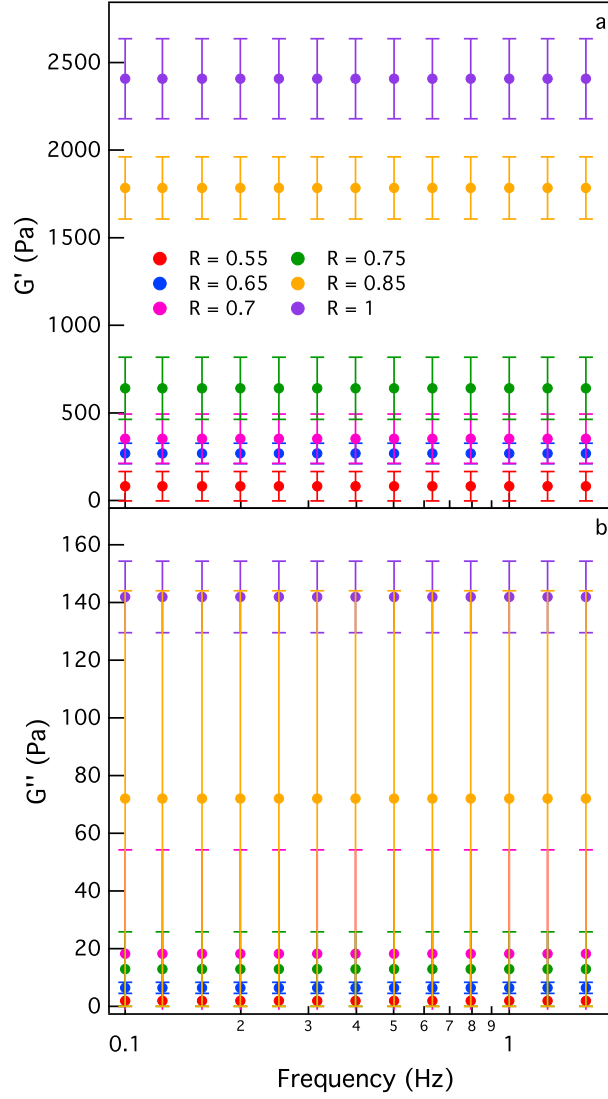Figure S1: Hydrogel swollen a) elastic (G') and b) loss (G'') moduli for different thiol:ene ratios, $R = \frac{thiol}{ene}$. The thiol:ene ratio is varied to make hydrogels with different stiffnesses to mimic elasticity of different tissues. The reported value is the average and the error is the standard deviation of three measurements.
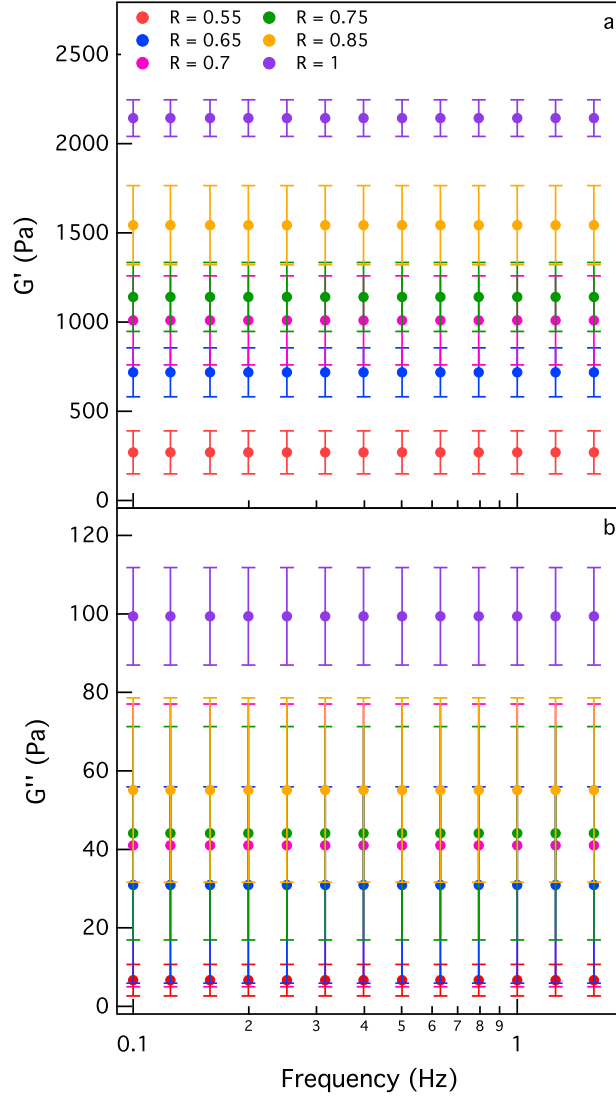
Figure S2: Hydrogel unswollen a) elastic (G') and b) loss (G'') moduli for different thiol:ene ratios, $R = \frac{thiol}{ene}$. The thiol:ene ratio is varied to make hydrogels with different stiffnesses to mimic elasticity of different tissues. The reported value is the average and the error is the standard deviation of three measurements.
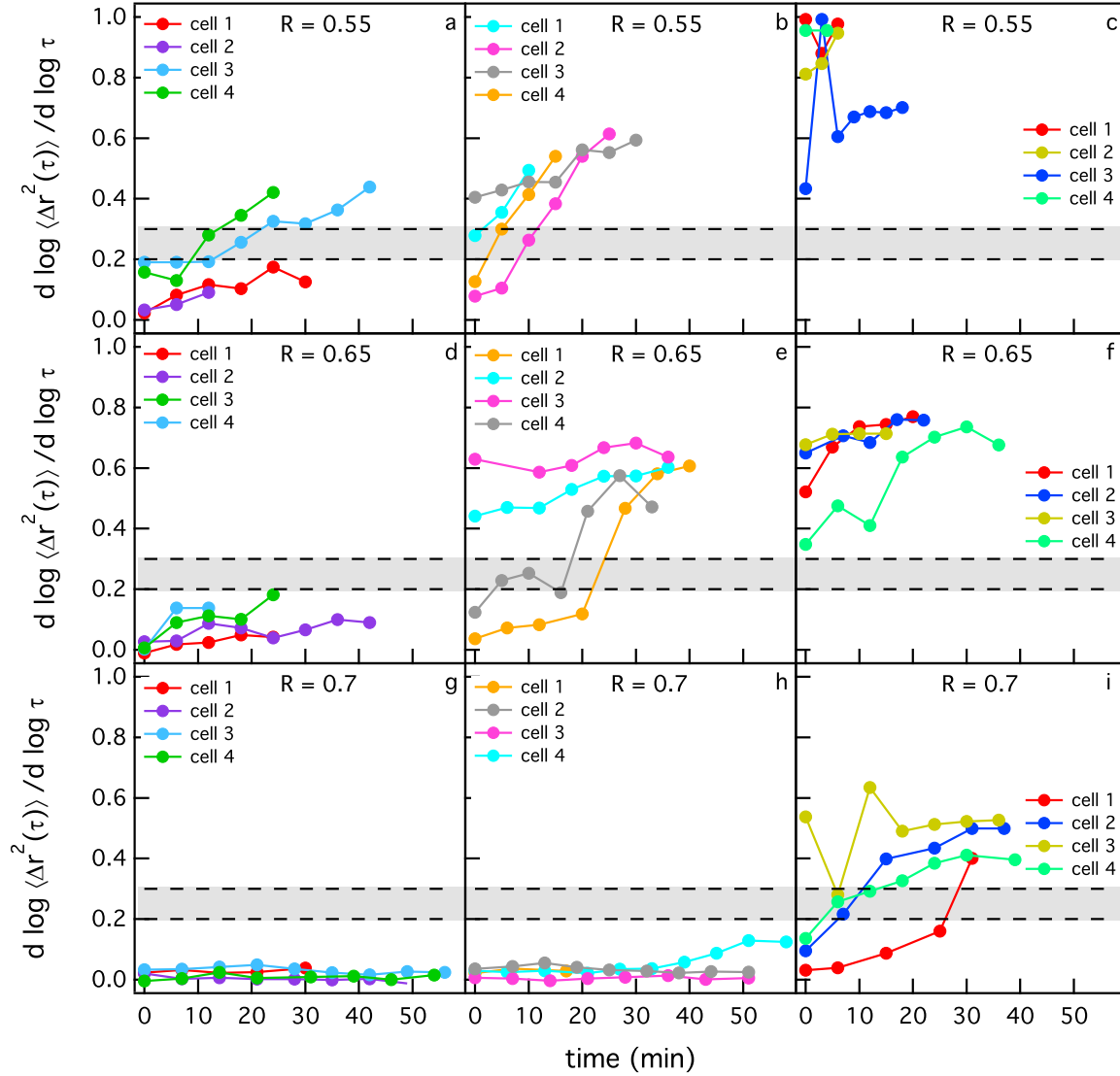
Figure S3: Changes in the logarithmic slope of mean-squared displacement, $\alpha = \frac{d\log\langle\Delta r^2(\tau)\rangle}{d\log\tau}$, over time for hMSCs encapsulated in (a-c) $R = 0.55$, (d-f) $R = 0.65$ and (g-i) $R = 0.7$. Each line represents the change in the value of α over time around a single hMSC. The left column is MPT data collected 3 *days* post-encapsulation, the middle column is 4 *days* post-encapsulation and the right column data 6 *days* post-encapsulation. R is the defined as $R = \frac{thiol}{ene}$.
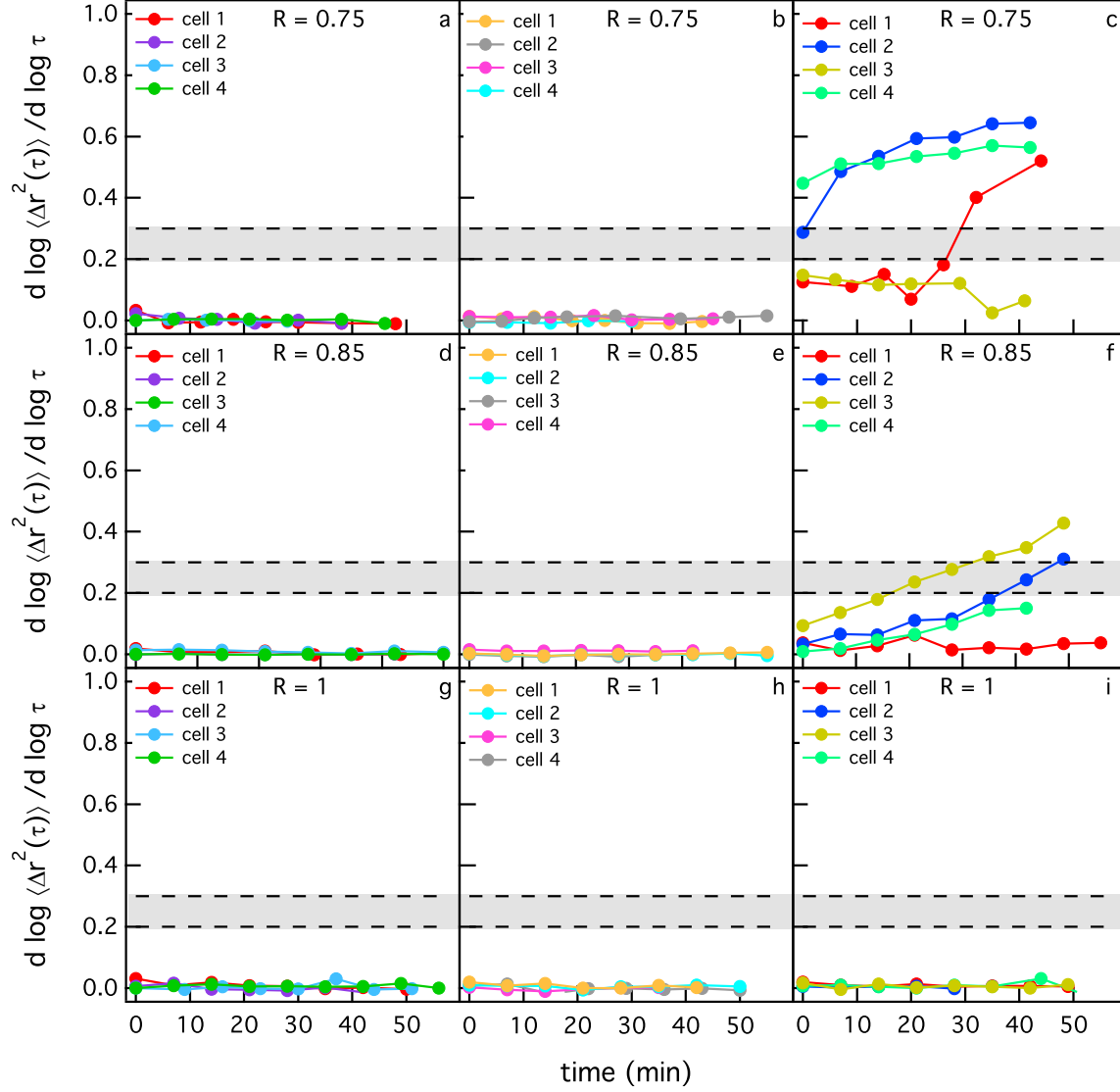
Figure S4: Changes in the logarithmic slope of mean-squared displacement, $\alpha = \frac{d\log\langle\Delta r^2(\tau)\rangle}{d\log\tau}$, over time for hMSCs encapsulated in (a-c) $R = 0.75$, (d-f) $R = 0.85$ and (g-i) $R = 1$. Each line represents the change in the value of α over time around a single hMSC. The left column is MPT data collected 3 *days* post-encapsulation, the middle column is 4 *days* post-encapsulation and the right column is 6 *days* post-encapsulation. R is defined as $R = \frac{thiol}{ene}$.
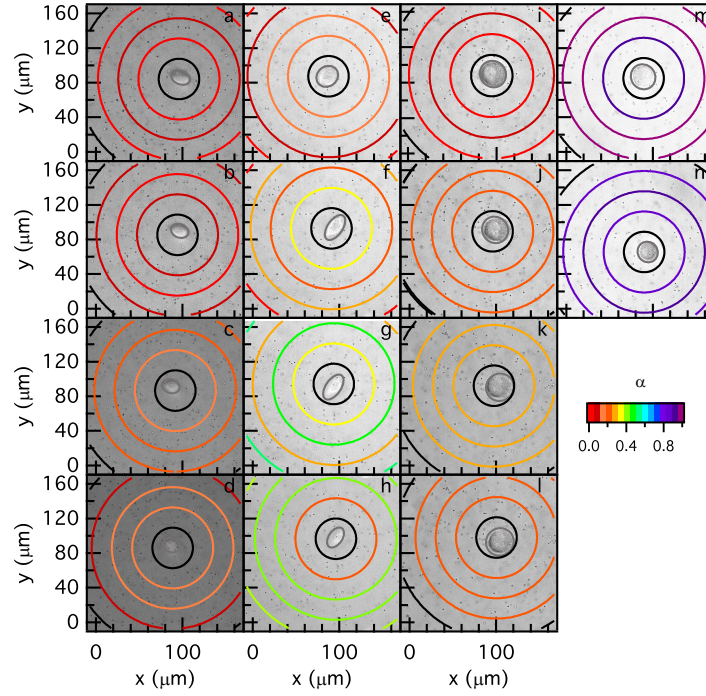
Figure S5: Spatial degradation profiles around hMSCs encapsulated in $R = 0.55$ hydrogels measured with MPT (a-h) 3 (i-l) 4 and (m-n) 6 *days* post-encapsulation. Two degradation profiles 3 *days* post-encapsulation are shown, which are (a-d) a uniform and (e-h) a no pattern degradation profile. (i-l) A uniform profile is measured 4 *days* post-encapsulation. (m-n) A degraded profile is measured 6 *days* post-encapsulation. MPT data are collected after locating the cell 3 *days* post-encapsulation at (a) 0, (b) 7, (c) 20, (d) 28, (e) 0, (f) 12, (g) 18 and (h) 24 *mins*, 4 *days* post-encapsulation at (i) 0, (j) 10, (k) 17 and (l) 22 *mins* and 6 *days* post-encapsulation at (m) 0 and (n) 3 *mins*. The color of each ring represents $\alpha = \frac{d\log\langle\Delta r^2(\tau)\rangle}{d\log\tau}$, which determines the state of the material in the scaffold.
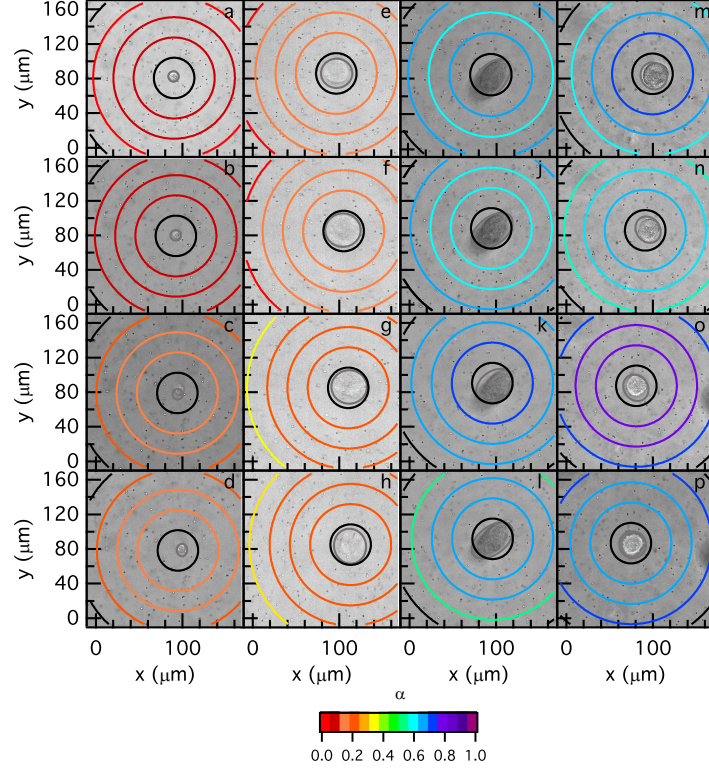
Figure S6: Spatial degradation profiles around hMSCs encapsulated in $R = 0.65$ hydrogels measured with MPT (a-d) 3 (e-l) 4 and (m-p) 6 *days* post-encapsulation. (a-d) A reverse reaction-diffusion profile is measured 3 *days* post-encapsulation. Two degradation profiles 4 *days* post-encapsulation are shown, which are (e-h) a uniform and (i-l) a degraded profile. In the uniform profile, in (g) and (h) the color of the outer ring is a higher α value then the inner ring. Based on our calculation these α values are not significantly significant and, therefore, this profile is a uniform degradation profile. (m-p) A degraded profile is measured 6 *days* post-encapsulation. Degraded profiles can have different spatial patterns at each time points of the experiment, but we have classified them as degraded since $\alpha > 0.6$ at the time that the cell is located for the entire pericellular region and this value does not change with time during data acquisition. MPT data are collected after locating the cell 3 *days* post-encapsulation at (a) 0, (b) 24, (c) 36 and (d) 42 *mins*, 4 *days* post-encapsulation at (e) 0, (f) 19, (g) 31, (h) 37, (i) 0, (j) 18, (k) 30 and (l) 36 *mins* and 6 *days* post-encapsulation at (m) 0, (n) 12, (o) 22 and (p) 27 *mins*. The color of each ring represents $\alpha = \frac{d \log \langle \Delta r^2(\tau) \rangle}{d \log \tau}$, which determines the state of the material in the scaffold.
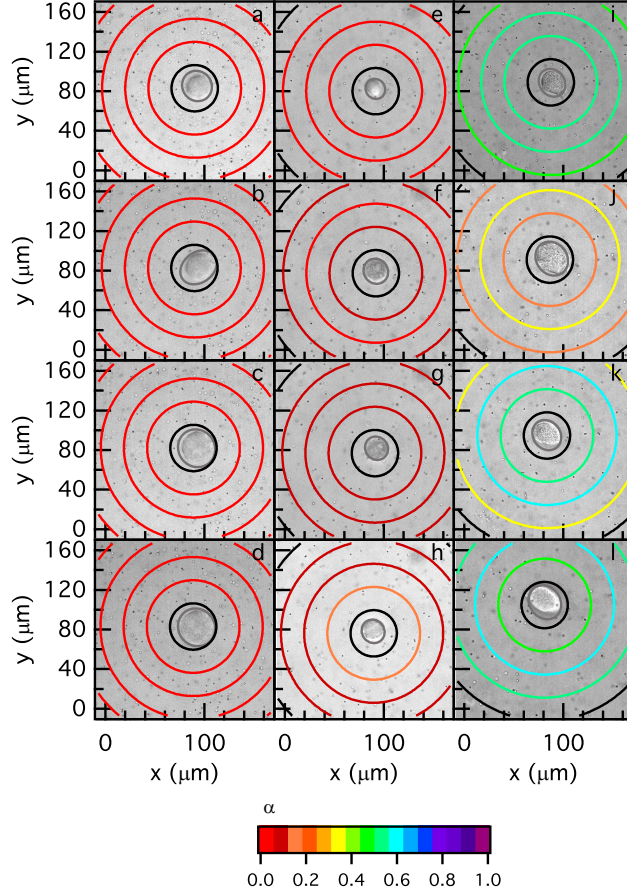
Figure S7: Spatial degradation profiles around hMSCs encapsulated in $R = 0.7$ hydrogels measured with MPT (a-d) 3 (e-h) 4 and (i-l) 6 *days* post-encapsulation. (a-d) A not degraded profile is measure 3 *days* post-encapsulation. (e-h) A uniform profile is measured 4 *days* post-encapsulation. (i-l) A no pattern profile is measured 6 *days* post-encapsulation. MPT data are collected after locating the cell 3 *days* post-encapsulation at (a) 0, (b) 14, (c) 35 and (d) 49 *mins*, 4 *days* post-encapsulation at (e) 0, (f) 22, (g) 30 and (h) 44 *mins* and 6 *days* post-encapsulation at (i) 0, (j) 6, (k) 24 and (l) 36 *mins*. The color of each ring represents $\alpha = \frac{d \log \langle \Delta r^2(\tau) \rangle}{d \log \tau}$, which determines the state of the material in the scaffold.
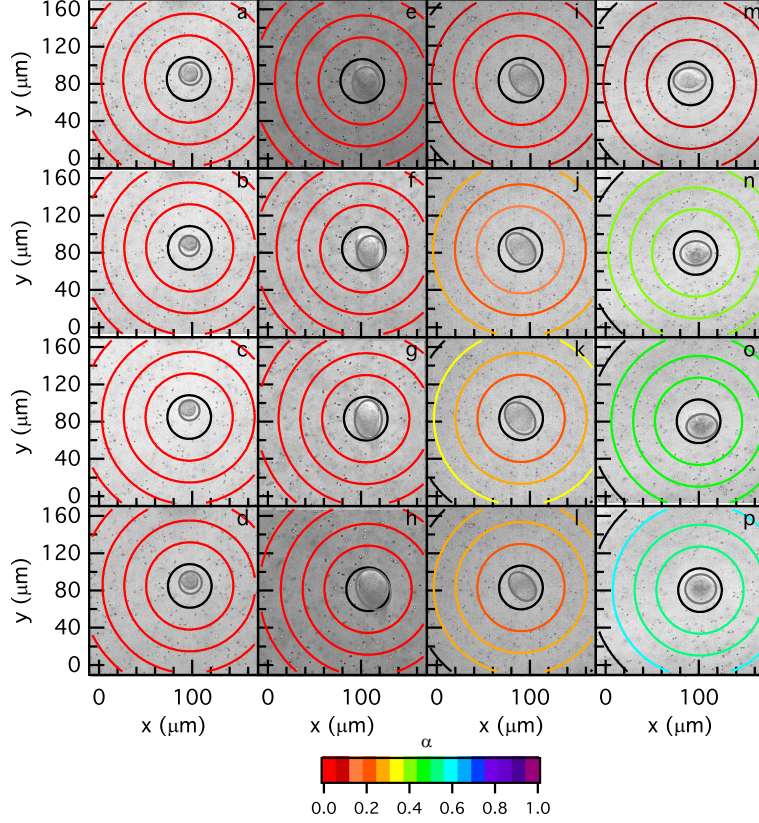
Figure S8: Spatial degradation profiles around hMSCs encapsulated in $R = 0.85$ hydrogels measured with MPT (a-d) 3 (e-h) 4 and (i-p) 6 *days* post-encapsulation. Not degraded profiles are measured (a-d) 3 and (e-h) 4 *days* post-encapsulation. Two degradation profiles 6 *days* post-encapsulation are shown, which are (i-j) a reverse reaction-diffusion and (m-p) a uniform degradation profile. MPT data are collected after locating the cell 3 *days* post-encapsulation at (a) 0, (b) 14, (c) 35 and (d) 49 *mins*, 4 *days* post-encapsulation at (e) 0, (f) 21, (g) 35 and (h) 49 *mins* and 6 *days* post-encapsulation at (i) 0, (j) 28, (k) 42, (l) 49, (m) 0, (n) 14, (o) 21 and (p) 42 *mins*. The color of each ring represents $\alpha = \frac{d \log \langle \Delta r^2(\tau) \rangle}{d \log \tau}$, which determines the state of the material in the scaffold.
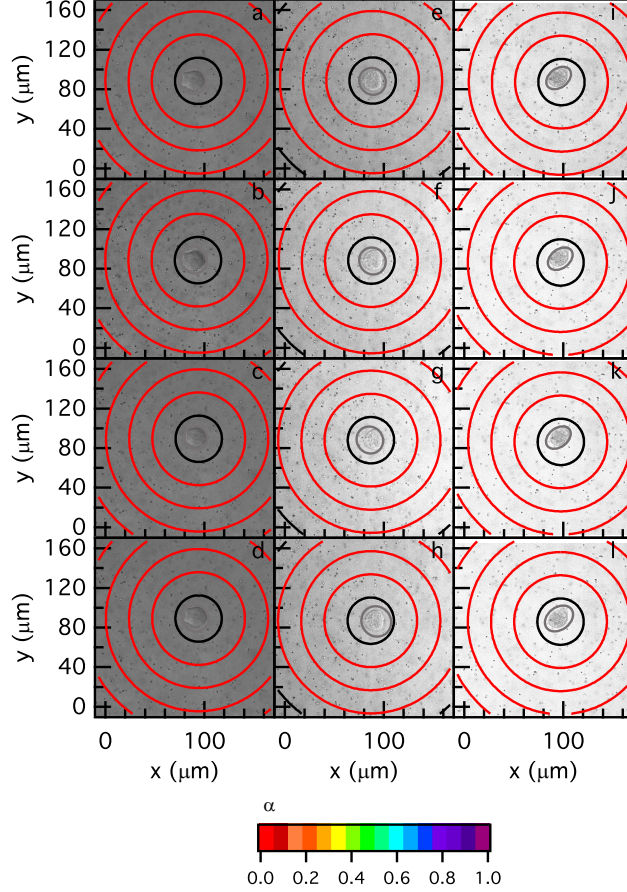
S10

Figure S9: Spatial degradation profiles around hMSCs encapsulated in $R = 1$ hydrogels measured with MPT (a-d) 3 (e-h) 4 and (i-p) 6 *days* post-encapsulation. All degradation profiles in this hydrogel scaffold are not degraded. MPT data are collected after locating the cell 3 *days* post-encapsulation at (a) 0, (b) 12, (c) 24 and (d) 48 *mins*, 4 *days* post-encapsulation at (e) 0, (f) 14, (g) 35 and (h) 49 *mins* and 6 *days* post-encapsulation at (i) 0, (j) 21, (k) 42 and (l) 56 *mins*. The color of each ring represents $\alpha = \frac{d \log \langle \Delta r^2(\tau) \rangle}{d \log \tau}$, which determines the state of the material in the scaffold.